Macromolecules

Article

pubs.acs.org/Macromolecules

Nonequilibrium Work Relations for Polymer Dynamics in Dilute Solutions

Folarin Latinwo[†] and Charles M. Schroeder*[,†,‡,§]

[†]Department of Chemical and Biomolecular Engineering, [‡]Department of Materials Science and Engineering, and [§]Center for Biophysics and Computational Biology, University of Illinois at Urbana—Champaign, Urbana, Illinois 61801, United States

ABSTRACT: Equilibrium and nonequilibrium free energies of complex fluids are fundamental quantities that can be used to determine a wide array of system properties. Recently, we demonstrated the direct determination of the equilibrium free energy landscape and corresponding elasticity of polymer chains from work calculations in highly nonequilibrium fluid flows.[1] In the present study, we further demonstrate the generality of this formalism by applying this method to polymeric systems driven by fluid flows with vorticity and for molecules with dominant intramolecular hydrodynamic interactions (HI). We employ Brownian dynamics simulations of double stranded DNA with fluctuating HI, and we analyze polymer dynamics and the resultant free energy calculations in the context of the nonequilibrium work relations. Furthermore, we investigate the role of HI on the work and housekeeping power required to maintain a polymer chain at a nonequilibrium steady-state in flow, and we consider the relationship between housekeeping power and polymer chain size. On the basis of the results in this study, nonequilibrium work relations appear to be a powerful set of tools that can be used to understand the behavior of polymeric systems and soft materials.

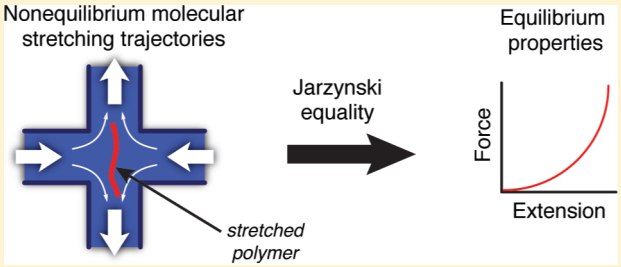

INTRODUCTION

Polymers are ubiquitous materials in modern society. During processing, polymer chains are exposed to nonequilibrium conditions that give rise to complex dynamics. A full description of the dynamic behavior of long chain macromolecules can be a challenging task. In the past, the nonequilibrium behavior of polymers in flow has been studied using a combination of bulk rheology, single polymer dynamics, kinetic theory, and simulations.[2−4] Bulk rheological experiments such as flow birefringence,[5] and light scattering[6,7] are used to infer information regarding polymer conformation orientation in flow, whereas single molecule techniques have allowed for the direct observation of polymers in shear flow,[8] planar extensional flow,[9,10] and two-dimensional mixed flows.[11] In this way, single molecule studies have uncovered intriguing information regarding the dynamic behavior of polymers at the molecular level. For example, observation of polymer dynamics in strong flows reveals distinct molecular stretching pathways and rich individualistic behavior.[9] In many cases, single molecule methods allow for the determination of the full distribution of polymer conformations at the molecular level, rather than the mean value of a bulk property. Experimental observation of chain dynamics in flow has been complemented by significant progress in computational modeling, including development of Brownian dynamics and Monte Carlo simulations.

In general, the modeling of nonequilibrium polymer dynamics using coarse-grained simulations follows a fairly structured approach. Model parameters based on polymer chemistry (e.g., elasticity, persistence length, contour length), solution conditions (e.g., Debye length, solvent quality), or both (e.g., longest polymer relaxation time) are chosen such that simulations accurately capture known (equilibrium) properties of molecules. Using this approach, the nonequilibrium dynamics of polymer chains are simulated using predetermined parameters, thereby revealing microstructual information and far-from-equilibrium properties such as chain stretch or solution stresses. Single molecule visualization and Brownian dynamics simulation of polymer chains provides a particularly powerful combination of complementary tools to study polymer dynamics.[4]

With this in mind, is it possible to approach nonequilibrium polymer dynamics from a fundamentally different perspective, one in which far-from-equilibrium properties of polymer chains are used to determine equilibrium fundamental materials properties such as elasticity? At first glance, this appears to be a daunting task for many reasons, including the highly dissipative nature of hydrodynamic forces in fluid flow. In this work, we show that equilibrium polymer properties such as stored elastic energy and polymer elasticity can be directly determined from polymer dynamics in a wide array of conditions, including fluid flows with vorticity and for polymer chains with dominant intramolecular hydrodynamic interactions (HI). In this way, rheological information can be used to determine characteristic properties that define specific polymeric systems. Determination of these fundamental properties

Received: May 8, 2013
Revised: August 14, 2013
Published: October 4, 2013

   dx.doi.org/10.1021/ma400961s | *Macromolecules* 2013, 46, 8345−8355

is enabled by nonequilibrium work relations that allow for calculation of equilibrium properties from far-from-equilibrium information.

Over the past decade, nonequilibrium work relations have been used in the field of biophysics in order to study short polymer chains of biological origin (e.g., RNA hairpins). Most of these experimental methods rely on single molecule techniques such as force spectroscopy (e.g., optical tweezers, AFM) in the absence of fluid flow. These methods typically require complex instrumentation with at least one end of the molecule tethered to a surface and the other attached to an optically trapped bead, AFM tip, or magnetic bead through which a conservative force is directly applied.[12] On the other hand, fluid flows can be used to generate substantial hydrodynamic forces on polymer molecules, which results in stretching and orientation of polymer chains in flow.[3,4,13,14] However, until recently, nonequilibrium work relations have not been applied to the field of complex fluids.

Recent advances in nonequilibrium statistical mechanics[15,16] via Jarzynski's equality (JE)[17,18] have enabled equilibrium properties to be determined from the work required to drive a process arbitrarily far from equilibrium. The Jarzynski equality is given as

$$e^{-\beta\Delta F} = \langle e^{-\beta w}\rangle = \int dw\, p(w) e^{-\beta w} \tag{1}$$

where ΔF is the free energy change between two states, w is the work done on the system during a process connecting the states, $\beta = 1/k_B T$ is the inverse Boltzmann temperature with k_B as Boltzmann's constant and T as absolute temperature, and $p(w)$ is the probability distribution associated with the work distribution w. In general, JE is a nonequilibrium work relation that enables the determination of free energy differences between two states from repeated nonequilibrium work measurements during an arbitrary process. In the original statement of the JE, the initial and final states of the system were taken to be equilibrium states.[17] However, the work relation has also been extended to nonequilibrium steady-states[19] and nonequilibrated states,[15] under certain circumstances. A sufficient condition for the application of the JE to nonequilibrium steady-states is that the steady-state distribution function ψ_{steady} can be described by a Boltzmann distribution such that $\psi_{steady} \propto \Phi \exp[-\beta H]$, where Φ is any arbitrary function and H is the position dependent Hamiltonian.[20]

Prior to the JE and related nonequilibrium work relations, free energy changes between two states were computed only for *reversible* processes such that

$$\Delta F = \langle w\rangle \tag{2}$$

In many cases, tremendous time scales are required to access these states in a reversible fashion. Alternatively, the free energy change associated with near equilibrium states is given by

$$\Delta F = \langle w\rangle - \frac{\beta}{2}\sigma^2 \tag{3}$$

where σ^2 is the variance of the work distribution from repeated work measurements, a result obtained from linear response theory.[21,22] In addition, for processes with Gaussian work distributions, which is the case near equilibrium or under the stiff spring approximation, it can be shown that eq 1 reduces to eq 3.[23] Since the development of the Jarzynski equality, nonequilibrium work relations have been extensively applied to biophysical systems[23−29] and quantum systems[30−34] using experiments and computer simulations. In biophysical applications, free energy changes between states were determined from pulling DNA and RNA hairpins using force spectroscopy in the absence of fluid flow over length scales ranging from tens of angstroms to hundreds of nanometers. In order to develop a practical framework to study complex fluids dynamics and rheology, however, nonequilibrium work relations need to be applied to systems driven by fluid flow.

Recently, we developed a framework to determine elasticity from single molecule polymer dynamics in vorticity-free linear flows.[1] In particular, we applied the nonequilibrium framework to study synthetic polymers and biopolymers stretched in tethered uniform and extensional flow, using both Brownian dynamics simulations and analysis of experimental data.[1] In this way, we calculated equilibrium free energy landscapes and force−extension relationships for free-draining chains of λ-DNA and polystyrene from their stretching trajectories in flow. However, realistic polymer chains are typically not free-draining molecules. In dilute solutions, polymer chains are affected by intramolecular hydrodynamic interactions (HI), wherein segments of a polymer affect solvent velocity, thereby perturbing the motion of nearby segments of the same polymer that are in close proximity.[10] Intramolecular HI is especially important for dynamics in the coiled state, wherein interior segments of the polymer chain are shielded from the full solvent flow field by outer segments of the polymer chain.

In general, the implications of HI can be significant especially for long and flexible polymer chains.[35−37] Regarding equilibrium chain dynamics, HI leads to enhanced diffusivities (D) and diminished longest relaxation times (τ_R) for a constant molecular weight (M). For example, the center-of-mass diffusion constant D and the longest relaxation time τ_R follow distinct scalings as a function of number of Kuhn segments (N_K) of the polymer chain, such that $D \sim N_K^{-1}$ and $\tau_R \sim N_K^2$ for free-draining chains following Rouse dynamics, while $D \sim N_K^{-0.5}$ and $\tau_R \sim N_K^{1.5}$ for hydrodynamically interacting chains in a θ-solvent following Zimm dynamics.[38,39] In the case of far-from-equilibrium dynamics, HI can lead to even more pronounced and interesting physics. For high molecular weight polymers, intramolecular HI leads to polymer conformation hysteresis in extensional flow,[10,13,36] while in confined geometries, HI results in distinct mobility and chain migration dynamics.[40−43] Although the effect of HI on chain dynamics is understood, the implication of HI on nonequilibrium work relations remains largely unknown.[44]

In addition to hydrodynamic interactions, vorticity plays a key role in polymer dynamics. For example, vorticity leads to characteristic tumbling dynamics of flexible and semiflexible polymer chains in shear flows.[45−49] Shear flow is a linear flow with equal contributions of pure rotation and pure deformation,[50] which results in an interesting interplay between polymer stretching, tumbling, and restretching events.[8,48,49] Recently, the dynamics of polymers in shear flow have been studied in the context of nonequilibrium work relations and corresponding fluctuation theorems,[51−53] albeit using single-mode Hookean dumbbell models of polymer chains. Hookean force relations provide a strictly linear elasticity, which results in unphysical behavior in strong flows.[3] From this view, prior work has applied nonequilibrium work relations to Hookean dumbbell models of polymer chains in shear flow, but results have largely been limited to the weak shear rate regime. Application of the JE to polymers in strong shear flow is of

dx.doi.org/10.1021/ma400961s | Macromolecules 2013, 46, 8345−8355

particular interest from a rheological and thermodynamic perspective.[53]

Here, we report the determination of fundamental materials properties by applying the JE to polymer chains in a wide range of linear flows. We use Brownian dynamics simulations to carefully extract the free energy landscape of polymer chains, which allows for the determination of chain elasticity for free-draining and nonfree-draining polymers in tethered uniform flow, planar extensional flow, and shear flow. In particular, we consider elastic models that describe synthetic polymer molecules such as polystyrene and biopolymers such as double stranded DNA. Finally, we make connections between nonequilibrium work quantities such as housekeeping power to well-known rheological quantities, and we derive expressions that deepen our understanding of this framework. In this way, we demonstrate the general applicability of using this new formalism in nonequilibrium statistical mechanics to elucidate fundamental properties from polymer dynamics.

BROWNIAN DYNAMICS SIMULATIONS AND WORK CALCULATIONS

Model Description. Polymers are modeled using a coarse-grained description of macromolecules, where chains are given by a series of N_b beads connected by massless springs. Beads serve as contact points with the fluid or centers of hydrodynamic drag, connected by $N = N_b - 1$ springs that prescribe the average elasticity of the molecules.[10,35,54] The motion of a polymer chain with fluctuating intramolecular hydrodynamic interactions is governed by a force balance on each bead and yields the stochastic differential equation:

$$\mathrm{d}\mathbf{r}_i = \left[\mathbf{u}(\mathbf{r}_i) + \frac{1}{k_\mathrm{B}T}\sum_{j=1}^{N_b}\mathbf{D}_{ij}\cdot\mathbf{F}_j + \sum_{j=1}^{N_b}\frac{\partial}{\partial\mathbf{r}_j}\cdot\mathbf{D}_{ij}\right]\mathrm{d}t + \sqrt{2}\sum_{j=1}^{i}\mathbf{B}_{ij}\cdot\mathrm{d}\mathbf{W}_j \tag{4}$$

where $\mathbf{r}_i$ is the position vector of bead i, $\mathbf{u}(\mathbf{r}_i)$ is the unperturbed fluid velocity at position $\mathbf{r}_i$, and $\mathbf{D}_{ij}$ is the diffusion tensor that satisfies a fluctuation−dissipation theorem such that:

$$\mathbf{D}_{ij} = \sum_{l=1}^{N_b}\mathbf{B}_{il}\cdot\mathbf{B}_{jl}^T \tag{5}$$

where $\mathbf{B}_{ij}$ is lower-triangular and represents the weighting factors, $\mathrm{d}\mathbf{W}_j$ is the vector representative of a Wiener process[55] with components chosen randomly from a Gaussian distribution with mean 0 and variance $\mathrm{d}t$, and $\mathbf{F}_j$ is the vector comprising the total nonhydrodynamic and non-Brownian forces acting on bead j. In modeling intrachain HI, there are two popular choices for the diffusion tensor: the Oseen−Burger (OB) and the Rotne−Prager−Yamakawa (RPY) tensor.[56] In both cases, the term $\sum_{j=1}^{N_b}(\partial/\partial\mathbf{r}_j)\cdot\mathbf{D}_{ij} = 0$, which greatly simplifies the force balance given by eq 4. We employ the RPY tensor in our simulations because it remains positive-semidefinite for all polymer chain configurations. The RPY tensor is given by:

$$\mathbf{D}_{ij} = \frac{k_\mathrm{B}T}{6\pi\eta_s a}\mathbf{I}_{ij}, \quad \text{if } i = j \tag{6a}$$

$$\mathbf{D}_{ij} = \frac{k_\mathrm{B}T}{8\pi\eta_s|\mathbf{r}_{ij}|}\mathbf{A}_{ij}$$

$$\mathbf{A}_{ij} = \begin{cases} \left[\left(1 + \frac{2a^2}{3|\mathbf{r}_{ij}|^2}\right)\mathbf{I}_{ij} + \left(1 - \frac{2a^2}{|\mathbf{r}_{ij}|^2}\right)\frac{\mathbf{r}_{ij}\mathbf{r}_{ij}}{|\mathbf{r}_{ij}|^2}\right], \\ \text{for } |\mathbf{r}_{ij}| \geq 2a, \quad \text{if } i \neq j, \\ \frac{|\mathbf{r}_{ij}|}{2a}\left[\left(\frac{8}{3} - \frac{3|\mathbf{r}_{ij}|}{4a}\right)\mathbf{I}_{ij} + \frac{\mathbf{r}_{ij}\mathbf{r}_{ij}}{4a|\mathbf{r}_{ij}|}\right], \\ \text{for} |\mathbf{r}_{ij}| < 2a, \quad \text{if } i \neq j \end{cases} \tag{6b}$$

where η_s is the solvent viscosity, a is the bead radius which is related to a hydrodynamic interaction parameter h^* such that $a = h^*((\pi k_B T)/H)^{1/2}$, $\mathbf{r}_{ij}$ is the vector displacement between beads i and j, and H is Hookean spring constant such that $H = ((3k_BT)/(N_{K,s}b_K^2))$, where $N_{K,s}$ is the number of Kuhn steps per spring and b_K is the Kuhn step size. Using this description, the contour length of the polymer chain is $L = (N_b - 1)N_{K,s}b_K$. It should be noted that $h^* = 0$ for free-draining chains, which implies that $\mathbf{D}$ is isotropic in the absence of HI.

In order to express eq 4 in dimesionless form, we define a characteristic time scale $t_s = \zeta/4H$, where ζ is the drag coefficient of each bead, a length scale $l_s = ((k_BT)/H)^{1/2}$, a force scale $F_s = (Hk_BT)^{1/2}$, and an energy scale $E_s = k_BT$. Furthermore, it is convenient to recast the force balance in eq 4 in terms of spring connector vectors $\mathbf{Q}_i \equiv \mathbf{r}_{i+1} - \mathbf{r}_i$ such that:

$$\mathrm{d}\mathbf{Q}_i = [Pe(\kappa\cdot\mathbf{Q}_i) + \sum_{j=1}^{N_b}(\mathbf{D}_{i+1,j} - \mathbf{D}_{i,j})\cdot\mathbf{F}_j^E]\mathrm{d}t + \sqrt{2}\,[\mathbf{B}_{i+1,i+1}\,\mathrm{d}\mathbf{W}_{i+1} + \sum_{j=1}^{i}(\mathbf{B}_{i+1,j} - \mathbf{B}_{i,j})\,\mathrm{d}\mathbf{W}_j] \tag{7}$$

where we have considered linear flows such that $\mathbf{u}(\mathbf{r}_i) = \boldsymbol{\kappa}\cdot\mathbf{r}_i$, where $\boldsymbol{\kappa}$ is the velocity gradient tensor. In eq 7, $Pe = Gt_s$ is the bead Péclet number, where G is the strain rate; $G = \dot{\epsilon}$ in extensional flow and $G = \dot{\gamma}$ in shear flow. Finally, $\mathbf{F}_i^E$ is the net entropic force on bead i and is given as

$$\mathbf{F}_i^E = \begin{cases} \mathbf{F}_1^s, & \text{if } i = 1 \\ \mathbf{F}_i^s - \mathbf{F}_{i-1}^s, & \text{if } 1 < i < N \\ -\mathbf{F}_{N-1}^s, & \text{if } i = N \end{cases} \tag{8}$$

where $\mathbf{F}_i^S = +(\partial/(\partial\mathbf{Q}_i))\phi^c$ is the entropic force in spring i, and ϕ^c is the connector potential. For modeling double stranded DNA, we employ the Marko-Siggia force-relation:[57]

$$\mathbf{F}_i^s = \frac{k_\mathrm{B}T}{b_K}\left[\frac{1}{2}\frac{1}{\left(1 - \frac{Q}{Q_o}\right)^2} - \frac{1}{2} + 2\frac{Q}{Q_o}\right]\frac{\mathbf{Q}_i}{Q} \tag{9}$$

For modeling synthetic polymers, we employ Cohen's Padé approximation[58] to the inverse-Langevin chain (ILC) function to represent the entropic elasticity between two beads:[39]

dx.doi.org/10.1021/ma400961s | Macromolecules 2013, 46, 8345−8355

$$\mathbf{F}_i^s = \frac{k_B T}{b_K}\left[\frac{3 - \left(\frac{Q}{Q_o}\right)^2}{1 - \left(\frac{Q}{Q_o}\right)^2}\right]\frac{\mathbf{Q}_i}{Q_0} \tag{10}$$

In both cases, $Q_o = N_{K,s}b_K$ is the maximum extensibility (contour length) of the spring connector, and $Q = |\mathbf{Q}_i|$ is the magnitude of the spring connector vector. The Marko−Siggia relation has been shown to accurately model the elasticity of double stranded DNA (dsDNA), while the inverse-Langevin function is commonly used as the elasticity of polystyrene.[54]

Nonequilibrium Work Definition. Jarzynski's equality relies on nonequilibrium work values for an arbitrary process.[17] Therefore, the application of JE to Brownian dynamics simulations of single polymer molecules stretched by flow requires an accurate definition of the work exerted by the fluid on the polymer in flow. In previous applications of the JE involving force spectroscopy (e.g., optical tweezers), work is defined simply as force exerted over a specified distance. For particles (and polymers) in flow, work is rigorously defined through the following relation:[1,51]

$$\mathrm{d}w \equiv \left[\frac{\partial}{\partial t}U + \sum_{i=1}^{N_b}\left(\mathbf{u}(\mathbf{r}_i)\cdot\frac{\partial}{\partial \mathbf{r}_i}U + \mathbf{f}_i\cdot[\dot{\mathbf{r}}_i - \mathbf{u}(\mathbf{r}_i)]\right)\right]\mathrm{d}t \tag{11}$$

where U is the net potential energy experienced by a particle, which is directly related to the connector potential ϕ^c in simulations and is explicitly independent of time, and $\mathbf{f}_i$ accounts for nonconservative forces other than hydrodynamic flow exerted on particles. Note that the applied work for nonconservative forces (e.g., solid−solid friction) can be expressed as $\mathbf{f}_i\cdot\mathrm{d}\mathbf{r}_i$. However, in our simulations, $\mathbf{f}_i = \mathbf{0}$. The first two terms on the right-hand side of eq 11 are the material (or convective) derivative of U, which describes the total time rate of change of the potential energy, analogous to the transport of momentum in fluid motion given by the Navier−Stokes equation.[50] It is convenient to recast eq 11 in dimensionless form in terms of spring connector vectors such that:

$$w = \int\left(\sum_{i=1}^{N} Pe(\boldsymbol{\kappa}\cdot\mathbf{Q}_i)\cdot\mathbf{F}_i^s\right)\mathrm{d}t \tag{12}$$

In this study, we define terminal states as given by a predefined molecular stretch or extension, such that the work done by the fluid is calculated in transitioning the polymer from an initial molecular extension to a final molecular extension. With this definition, the free energy change between states (defined by constant molecular extensions) is determined by applying JE in dimensionless form

$$\Delta F = -\ln\left[\frac{1}{N_t}\sum_{k=1}^{N_t}\exp(-w_k)\right] \tag{13}$$

where N_t is the total number of trajectories in the ensemble exponential average. The number of trajectories required to yield reasonable estimates of the free energy change between states depends on the dissipated work $\langle w_d\rangle = \langle w\rangle - \Delta F$.[59] This number becomes prohibitively large when $\langle w_d\rangle \gg k_B T$, which can limit the application of JE to microscopic systems.[24] As discussed below, strategies have been developed to ensure that the work calculation is tractable.

Algorithm. In solving the dynamic force balance given by eqs 7−10, we employ a highly efficient predictor−corrector method to calculate the conformational changes in the polymer molecule as represented by the spring connector vectors. We follow closely the algorithm originally proposed by Somasi et al.[60] that has been adapted to simulations with fluctuating HI[54] and excluded volume (EV).[10]

At each time step, the algorithm begins with a predictor step, which is a simple Euler method to estimate the spring connector vectors at a later time $t + \Delta t$ given the connector vectors at time t:

$$\mathbf{Q}_i^{*,t+\Delta t} = [Pe(\boldsymbol{\kappa}\cdot\mathbf{Q}_i^t) + \sum_{j=1}^{N_b}(\mathbf{D}_{i+1,j}^t - \mathbf{D}_{i,j}^t)\cdot\mathbf{F}_j^{s,t}]\Delta t + \sqrt{2}[\mathbf{B}_{i+1,i+1}^t\cdot\mathrm{d}\mathbf{W}_{i+1}^t + \sum_{j=1}^{i}(\mathbf{B}_{i+1,j}^t - \mathbf{B}_{i,j}^t)\cdot\mathrm{d}\mathbf{W}_j^t] \tag{14}$$

where $\mathbf{Q}_i^{*,t+\Delta t}$ is the Euler prediction for the connector vector of spring i at time $t + \Delta t$. Next, we employ a correction based on the predicted connector vectors such that

$$\begin{aligned}\bar{\mathbf{Q}}_i^{t+\Delta t} + ((\mathbf{D}_{i+1,i+1}^t - \mathbf{D}_{i,i}^t)\cdot\bar{\mathbf{F}}_i^{s,t+\Delta t})\Delta t &= \left[\frac{1}{2}Pe(\kappa\cdot\mathbf{Q}_i^t + \kappa\cdot\mathbf{Q}_i^{*,t+\Delta t}) + (\mathbf{D}_{i+1,i+1}^t - \mathbf{D}_{i,i}^t)\cdot\mathbf{F}_i^{s,t}\right. \\ &\left. + \sum_{j=1}^{N_b}(\mathbf{D}_{i+1,j}^t - \mathbf{D}_{i,j}^t)\cdot\mathbf{F}_j^s\right]\Delta t + \sqrt{2}[\mathbf{B}_{i+1,i+1}^t\cdot\mathrm{d}\mathbf{W}_{i+1}^t \\ &+ \sum_{j=1}^{i}(\mathbf{B}_{i+1,j}^t - \mathbf{B}_{i,j}^t)\cdot\mathrm{d}\mathbf{W}_j^t]\end{aligned} \tag{15}$$

where $\mathbf{F}_j^s = \bar{\mathbf{F}}_j^{s,t+\Delta t}$ if $j < i$; else $\mathbf{F}_j^s = \mathbf{F}_j^{s,t}$, and $\bar{\mathbf{Q}}_i^{t+\Delta t}$ is the corrected spring connector i. The quantity $|\bar{\mathbf{Q}}_i^{t+\Delta t}|$ is first determined by solving a cubic equation derived from eq 15 that can be expressed differently for models of polystyrene[54] and DNA[10] based on their respective force-relations. By solving the cubic equation, the corrected estimate $\bar{\mathbf{Q}}_i^{t+\Delta t}$ is obtained. In writing eq 15, we add two diagonal terms involving $\mathbf{D}^t$ on both sides to avoid breaking the summation so as to conveniently determine $\bar{\mathbf{Q}}_i^{t+\Delta t}$ implicitly. Finally, the third step is an iterative determination of spring connector vector i given by:

$$\begin{aligned}\mathbf{Q}_i^{t+\Delta t} + ((\mathbf{D}_{i+1,i+1}^t - \mathbf{D}_{i,i}^t)\cdot\mathbf{F}_i^{s,t+\Delta t})\Delta t &= [\frac{1}{2}Pe(\boldsymbol{\kappa}\cdot\mathbf{Q}_i^t + \boldsymbol{\kappa}\cdot\bar{\mathbf{Q}}_i^{t+\Delta t}) + (\mathbf{D}_{i+1,i+1}^t - \mathbf{D}_{i,i}^t)\cdot\bar{\mathbf{F}}_i^{s,t+\Delta t} \\ &+ \sum_{j=1}^{N_b}(\mathbf{D}_{i+1,j}^t - \mathbf{D}_{i,j}^t)\cdot\mathbf{F}_j^s]\Delta t + \sqrt{2}[\mathbf{B}_{i+1,i+1}^t\cdot\mathrm{d}\mathbf{W}_{i+1}^t \\ &+ \sum_{j=1}^{i}(\mathbf{B}_{i+1,j}^t - \mathbf{B}_{i,j}^t)\cdot\mathrm{d}\mathbf{W}_j^t]\end{aligned} \tag{16}$$

where $\mathbf{F}_j^{s,t} = \mathbf{F}_j^{s,t+\Delta t}$ if $j < i$; else $\mathbf{F}_j^s = \bar{\mathbf{F}}_j^{s,t+\Delta t}$. We use eq 16 to determine the spring connector vectors $\mathbf{Q}_i^{t+\Delta t}$ for all N springs. For the iterative step, we use a convergence criterion given by ε_c:

dx.doi.org/10.1021/ma400961s | Macromolecules 2013, 46, 8345−8355

$$\varepsilon_c > \sqrt{\sum_{i=1}^{N} (\mathbf{Q}_i^{t+\Delta t} - \bar{\mathbf{Q}}_i^{t+\Delta t})^2} \tag{17}$$

If the convergence criterion is not satisfied, then the values of $\mathbf{Q}_i^{t+\Delta t}$ are copied into $\bar{\mathbf{Q}}_i^{t+\Delta t}$, and the algorithm steps are repeated in eq 16 until the condition in eq 17 is satisfied. Upon convergence, the set of spring connectors $\mathbf{Q}_i^{t+\Delta t}$ is finally determined. We typically set ε_c to 10^{-6} in our simulations.

In this algorithm, we have assumed $\mathbf{D}_{ij}$ and $\mathbf{B}_{ij}$ are constant during each time step Δt. This assumption is reasonable for small Δt as demonstrated by Jendrejack et al.[61] It should be noted that this assumption is unnecessary for $\mathbf{D}_{ij}$ in simulating free-draining chains, because by definition, free-draining chains have constant $\mathbf{D}_{ij}$. For hydrodynamically interacting chains, the elements $B_{\alpha\beta}$ of weighting factors $\mathbf{B}_{ij}$ are determined at the start of each time step via a Cholesky decomposition[62] on the elements $D_{\alpha\beta}$ of $\mathbf{D}_{ij}$[54,56] such that

$$B_{\alpha\alpha} = (D_{\alpha\alpha} - \sum_{\gamma=1}^{\alpha-1} \sigma_{\alpha\gamma}^2)^{1/2}$$

$$B_{\alpha\beta} = \frac{1}{\sigma_{\beta\beta}}(D_{\alpha\beta} - \sum_{\gamma=1}^{\beta-1} \sigma_{\alpha\gamma}\sigma_{\beta\gamma})^{1/2}, \quad \text{if } \alpha > \beta$$

$$B_{\alpha\beta} = 0, \quad \text{if } \alpha < \beta \tag{18}$$

where α, β, γ represent the row and column positions of the composite tensors $\mathbf{D}$ and $\mathbf{B}$. As implemented, the Cholesky decomposition is an $O(N^3)$ operation, where N represents the number of rows in $\mathbf{D}$. Other more efficient computational methods have been developed, including an $O(N^{2.25})$ method based on Chebyshev polynomials developed by Fixman,[63] which is efficient especially for chains with significant excluded volume.[10,61] More recently, even more efficient algorithms have been developed, including $O(N \log N)$[64] and $O(N)$[65] methods, though these are well-suited for simulations of polymers in confined geometries.

On the basis of the work definition in eq 12, the work dw exerted by the fluid on the polymer during a time step Δt depends only the spring connector vectors $\mathbf{Q}_i^t$ and the elasticity in the springs $\mathbf{F}_j^{s,t}$. Therefore, once the single trajectories of the polymer are known, the work done by the fluid can be calculated. The work computed for a trajectory k is given by:

$$w_k = \sum_{n=0}^{N_e} \sum_{i=1}^{N} Pe(\boldsymbol{\kappa}\cdot\mathbf{Q}_i^{t+n\Delta t})\cdot\mathbf{F}_i^{s,t+n\Delta t}\Delta t \tag{19}$$

where $t = 0$ at the beginning of the simulation, and N_e is the number of time steps in simulating trajectory k. As an aside, we note that the work calculation can also be performed using the hydrodynamic drag exerted by the fluid on the polymer chain, which is useful in analyzing experimental data.[1] In brief, the work definition utilized in the analysis of single-molecule experimental data is of the same functional form as in eqs 11 and 19. However, in the work expression used in the experimental analysis, the spring force is replaced by the hydrodynamic drag force using Zimm and slender-body theory.[1] Nevertheless, in this study, we use the work definition given by eq 12. When considering the work done by the fluid to stretch a polymer to predefined extension, the calculation is terminated at the first instance that the chain reaches the final extension; therefore, N_e varies for each trajectory due to the stochasticity associated with the Brownian forces in thermal motion. When considering housekeeping power, N_e is constant for all trajectories because we are concerned with the rate of the average work done over all trajectories *after* the molecule has reached an average steady-state (see section Housekeeping Power). Indeed, it is this consideration that enables us to relate the housekeeping power to viscometric functions by relying on the assumption of ergodicity.[1]

Stratification. Processes driven by fluid flow result in highly nonequilibrium conditions, thereby generating large amounts of dissipated work. In applying the JE to polymer molecules in flow, we employ a strategy known as stratification to overcome the limitations associated with highly dissipative processes driving overall large free energy changes.[66] We divide a process associated with a large free energy change ΔF_{tot} into N_{tot} subprocesses with smaller free energy changes, and we determine the work distribution $p(w_i)$ for each i subprocess. We then apply the JE to each subprocess to determine the associated free energy change ΔF_i. Because free energy is a thermodynamic state variable and is additive,[67] we can determine the total free energy change ΔF_{tot} by summing over the subprocesses such that $\Delta F_{tot} = \sum_{i=1}^{N_{tot}} \Delta F_i$. Moreover, determination of the total free energy change using this approach is generally convenient, because it allows the free energy landscape to be mapped as a function of molecular extension, which define our subprocesses.

We employ two methods in applying the stratification strategy to our calculations. In strategy I, we apply small successive step functions to the flow strength and allow a polymer molecule to first reach its average steady-state extension at each successive flow rate.[1] In strategy II, we apply a large step function to the flow strength and calculate the work required to transition between successive predefined molecular extensions. Both strategies are valid for work calculations, because we have defined our terminal states by molecular extension. In brief, we note that the equilibrium statement of the JE requires that the initial states be "equilibrated". This requirement is inherently satisfied in typical bead−spring models of polymeric materials because the chain elasticity *at all times* depends only on the molecular extension of the polymer chain. Furthermore, it should be noted that in both cases, the final states are defined by a fixed molecular extension, but we anticipate that strategy II will yield larger values of dissipated work due to the larger overall step in flow strength.

Housekeeping Power. Calculation of the work exerted by the fluid to stretch a polymer chain enables the determination of the equilibrium free energy landscape and elasticity. In this case, the work done by the fluid on the polymer is computed from time zero until the first time the polymer reaches a predefined molecular stretch. In addition to this calculation, it also is instructive to consider the work exerted by the fluid to maintain an average steady-state stretch, which is the work required to maintain an average nonequilibrium molecular extension in flow. Here, we define the housekeeping power (or applied power) as the rate of work performed by an external agent to maintain a polymer chain at a given average steady-state.[1,51] There is a sharp contrast between the case where a molecule is maintained at an average steady-state by conservative forces and the case where it is maintained by nonconservative forces, such as those encountered in hydrodynamic flows. For conservative forces, the applied power $P \equiv \langle \dot{w} \rangle$ is exactly zero, which is indicative of thermodynamic

dx.doi.org/10.1021/ma400961s | *Macromolecules* 2013, 46, 8345−8355

equilibrium. For hydrodynamic flows involving dissipative forces, P is a nonzero constant for steady flows and is intimately related to bulk polymer viscometric functions for dilute polymer solutions in linear flows.[1] In this work, we carefully investigate the effect of HI and vorticity on the housekeeping power for polymers in hydrodynamic flows.

RESULTS AND DISCUSSION

Free Energy Calculations in Flow. As a starting point, we determined the work required to stretch polymers in planar extensional flow. To begin, we simulated the dynamics of λ-DNA in flow using a free-draining dumbbell model, where $h^* = 0$ and $N_b = 2$. For over 15 years, λ-DNA has been used as a model polymer chain in single polymer experiments; λ-DNA labeled with intercalating dyes such as YOYO-1 is typically considered to have a contour length $L = 21$ μm, Kuhn step size $b_K = 132$ nm, and approximately $N_K = 159$ Kuhn steps.[4] We calculate the work done by the fluid to stretch a single polymer chain from an initial molecular extension (state a) to a predefined final molecular extension (state b). After a given polymer molecule reaches a predefined final state b, work calculations are halted for the trajectory. After the stretching event has concluded, it may be envisioned that the molecule is maintained at state b by a conservative force such that no additional work is performed on the molecule after reaching the final state; however, this is merely a construct to conceptualize the process.

Representative transient work values and the corresponding ensemble average of the work performed by the fluid to stretch λ-DNA during a particular event are shown in Figure 1. During this stretching event, λ-DNA is transitioned from a fractional extension $x/L = 0.32$ (state a) to $x/L = 0.38$ (state b) in planar extensional flow at a flow strength of $Wi = 0.63$. In determining the work distribution w required to stretch a polymer from the initial to final state, we only focus on the work required to reach the final extension. Therefore, the incremental work done by the fluid is zero after a given molecular trajectory reaches state b, which results in apparent plateaus in transient work values for single polymers shown in Figure 1. Our results show that different polymer chains reach their final extension (state b) at different times, which is consistent with a stochastic stretching process, thereby yielding a distribution of work values.

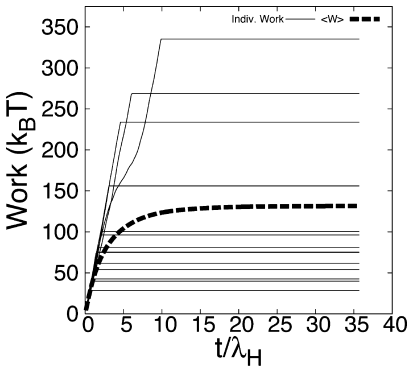

Figure 1. Transient work trajectories for stretching λ-DNA in extensional flow at $Wi = 0.63$. In this case, polymer molecules are stretched from a fractional extension $x/L = 0.32$ to 0.38 at a constant Wi. Thin lines represent work trajectories from individual polymer chains, and thick lines represent ensemble average work.

To further understand the origin of the work distribution for the process shown in Figure 1, we examine transient work trajectories for single chains responding to an imposed fixed flow rate (Figure 2). Overall, we observe two general classes of stretching events, as interpreted through transient work values: (1) trajectories with accumulated work values less than the average work and (2) trajectories with accumulated work values much greater than the average work. A molecular trajectory with a work value less than the average work is shown in Figure 2a. Stretching trajectories that yield small work values typically correspond to processes that are strongly dominated by stretching events, with few contracting events during the process. However, larger work values correspond to trajectories where the molecule spends a significant time contracting, which is interesting given that the overall process is a stretching event (Figure 2, parts b and c). During a molecular contraction event

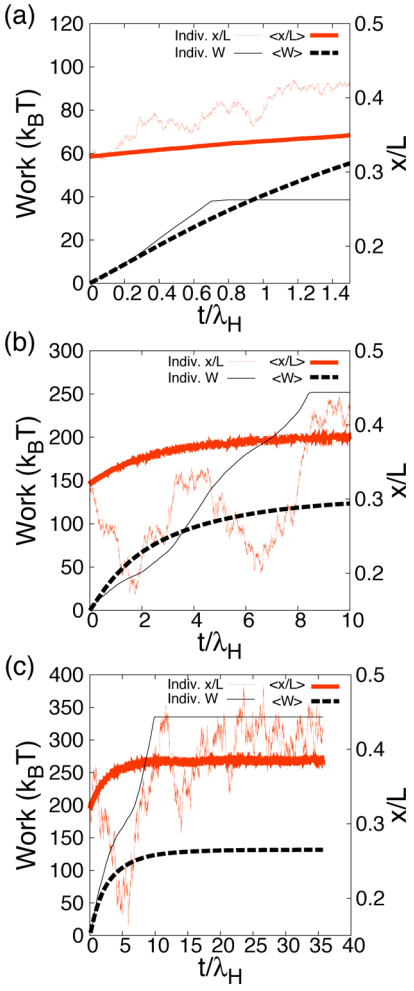

Figure 2. Transient work trajectories and corresponding transient molecular stretch for a free-draining polymer dumbbell model of λ-DNA in extensional flow at $Wi = 0.63$, where molecules stretched from $x/L = 0.32$ to 0.38. Thin lines represent trajectories from single polymer chains, and thick lines represent ensemble average quantities. (a) Trajectory for a process where the work done by the fluid on the molecule is less than average transient work. (b) Trajectory for a process where the work done by the fluid on the molecule is greater than average transient work. (c) Trajectory for a process where the work done by fluid on the molecule is significantly greater than average transient work.

dx.doi.org/10.1021/ma400961s | Macromolecules 2013, 46, 8345−8355

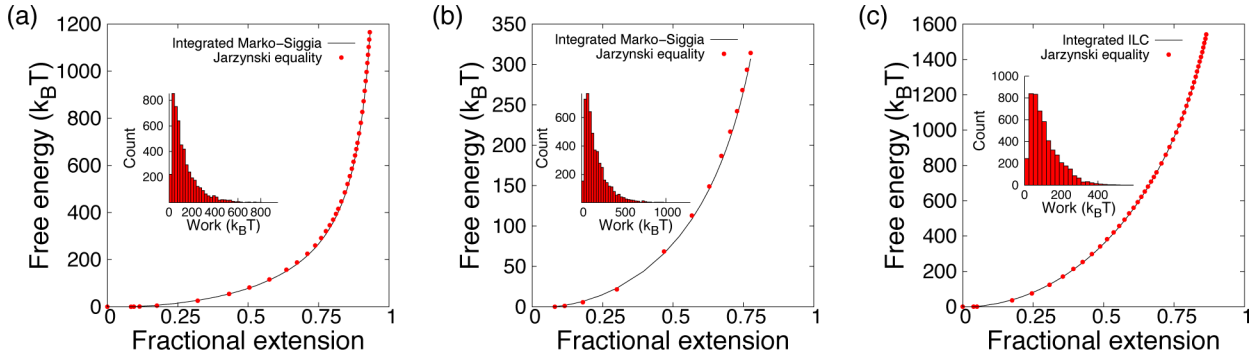

Figure 3. Equilibrium free energy landscape for λ-DNA (contour length, $L \approx 21$ μm) and polystyrene ($L \approx 1.2$ μm) determined from nonequilibrium dynamic simulations in general flows using the JE. The free energy at zero extension is defined as the reference state or zero energy. (a) Energy landscape for DNA molecules stretched in planar extensional flow. (Inset) Histogram showing distribution of work values required to stretch DNA molecules from $Wi = 0.59$ to $Wi = 0.63$, corresponding to a change in fractional extension from $x/L \approx 0.32$ to 0.38. (b) Energy landscape for DNA molecules stretched in tethered uniform flow. (Inset) Histogram showing distribution of work values required to stretch DNA molecules from $Pe = 8$ to $Pe = 9$, corresponding to a change in fractional extension from $x/L \approx 0.63$ to 0.65. (c) Energy landscape for PS molecules stretched in planar extensional flow. (Inset) Histogram showing distribution of work values required to stretch PS molecules from $Wi = 0.44$ to $Wi = 0.49$, corresponding to a change in fractional extension from $x/L \approx 0.06$ to 0.13.

in flow, the transient work increases in a concave-down manner because the incremental work decreases relative to a pure instantaneous stretching event. We note that the contraction event is due to the stochastic nature of single polymer dynamics at the imposed fixed flow rate. Nevertheless, the fluid continues to do work on the polymer chain, and the transient work continues to increase with a positive slope. On the other hand, during molecular stretching events, incremental work values generally increase relative to static stretch or contraction events, thereby yielding a concave-up shape of the transient work. Many individual stretching trajectories exhibit both contraction and stretching events, as shown in Figure 2b.

In this study, the system is defined as a polymer molecule at a fixed molecular extension. Here, we consider dynamic processes wherein a molecule is stretched from an initial molecular extension to a predefined final molecular extension by an imposed flow field. After determining the work distribution for a dynamic process, the JE can be applied to calculate the free energy difference for the given process (Figure 3). In particular, we divide a large process into a set of smaller subprocesses using the method of stratification. In this way, we can apply the JE using the work distribution for each subprocess (as given by eq 1), and then sum the energies together to determine the free energy change for a large process. For example, we determined the work distribution for the dynamic process shown in Figure 1 by building a histogram of work done by the fluid to stretch λ-DNA from $x/L = 0.32$ to 0.38 at a flow strength of $Wi = 0.63$ over several realizations (inset of Figure 3a). In an analogous manner, simulations of several subprocesses are performed for different flow strengths. Using this approach, we can determine the entire *equilibrium* free energy landscape of λ-DNA as a function of molecular extension, remarkably over 3 orders of magnitude in energy, as shown in Figure 3a. Interestingly, the free energy change associated with molecular transitions between states of *constant molecular extension* correspond exactly to the stored elastic energy in polymer chain.[1] In a second scenario, the system could be defined as a polymer molecule maintained in flow at a fixed flow strength or *Wi*. In this case, the dynamic process involves transitioning the system in a finite protocol from an initial *Wi* (state a) to a final *Wi* (state b). For this process, the work definition is entirely different from that in eqs 11 and 19. Furthermore, the application of Jarzynski equality to this scenario allows for the determination of a fundamentally different energy landscape altogether; this is subject of future work. Nevertheless, the present method considers states of constant molecular extension, and by using this method, we can determine the free energy difference to be within ± 1 k_BT of the analytic value obtained from integrating the Marko−Siggia force relation.

We further validated our method by studying the stretching dynamics of polymers in other flows. In addition to determining the stored elastic energy from stretching DNA in planar extensional flow, we also simulated the stretching dynamics of λ-DNA in uniform flow using a free-draining dumbbell model. In this simulation, one terminus of the polymer chain is tethered to a fixed position in the flow field. The inset in Figure 3b shows the work distribution for a subprocess in which a molecule is stretched from a fractional extension $x/L = 0.63$ to 0.65 in a uniform flow at a flow strength of $Pe = 9$. By applying the JE and employing the strategy of stratification, we are able to determine the free energy landscape of λ-DNA in uniform flow as shown in Figure 3b. Beyond applying our method to extract the equilibrium free energy landscape of biopolymers from stretching trajectories in flow, we further validated our approach by studying the stretching dynamics of polystyrene (PS) molecules in planar extensional flow. Figure 3c shows the equilibrium free energy landscape determined from applying the JE to work distributions obtained from the analysis of simulated free-draining stretching trajectories of PS molecules (contour length $L = 1.2$ μm) in planar extensional flow. The inset in Figure 3c shows a typical work distribution for a subprocess in which a PS molecule is stretched from a fractional extension $x/L = 0.06$ to 0.13 in a planar extensional flow at a $Wi = 0.49$. Overall, our results from the analysis of PS molecules in flow are in good agreement with the analytic stored elastic energy obtained by directly integrating the Padé approximation to the inverse-Langevin chain (ILC) relation with respect to molecular extension.

Free energy calculations demonstrate that the JE is applicable to free-draining models of polymer chains in vorticity-free linear flows. The equations of motion describing free-draining models of polymer chains are characterized by additive stochasticity. However, for models of polymer chains that

dx.doi.org/10.1021/ma400961s | *Macromolecules* 2013, 46, 8345−8355

incorporate fluctuating HI, the equations of motion are characterized by multiplicative stochasticity.[55] In order to demonstrate the robustness of our framework in the presence of HI, and therefore multiplicative stochasticity, we perform free energy calculations for multibead−spring models with fluctuating HI. In particular, we simulate the dynamics of λ-DNA using a multibead model with $h^* = 0.12$ and $N_b = 10$, parameters which are similar to prior work on λ-DNA.[68] Here, we employ the stratification strategy II, wherein a large step function in strain rate is applied, and the work done by the fluid to stretch a polymer to a predefined molecular extension is determined. This strategy is especially advantageous in that single chains are not held or maintained at their corresponding average nonequilibrium steady-state extension before stepping to the next the flow strength. This approach is particularly convenient due to the significant computational expense for simulation polymer chains with fluctuating HI.

We determined the *equilibrium* free energy for polymer chains modeled using coarse-grained multibead−spring chains with fluctuating HI (Figure 4). Parts a and b of Figure 4 show

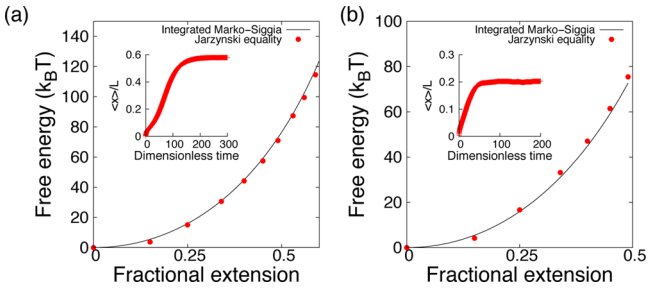

Figure 4. Equilibrium free energy landscape from multibead−spring model with fluctuating HI for λ-DNA in general flows using the JE with stratification Strategy II. The free energy at zero extension is defined as the reference state or zero energy. (a) Energy landscape for molecules stretched in extensional flow at $Wi = 0.8$. (Inset) Corresponding transient ensemble average fractional extension. (b) Energy landscape for molecules stretched in shear flow at $Wi = 0.8$. (Inset) Corresponding transient ensemble average fractional extension.

the free energy landscape of λ-DNA determined using stratification strategy II at $Wi = 0.8$ in planar extensional flow and shear flow, respectively. In strategy II, a molecule is stretched from a coiled state (equilibrated under no flow) to a final average stretched state at a given flow strength or Wi. The insets of parts a and b of Figure 4 show the corresponding transient trajectory of the ensemble average molecular extension of λ-DNA at $Wi = 0.8$ in an imposed extensional flow and shear flow, respectively. In applying strategy II, we determine the work done by the fluid as a molecule transitions between predefined molecular extensions which prescribe the subprocesses. In planar extensional flow, we observe that the free energy landscape can be determined up to a molecular extension that corresponds to the final average molecular extension reached by the polymer (Figure 4a). Interestingly, in shear flow, we observe that the free energy landscape can be determined significantly beyond the molecular extension that corresponds to the final average extension reached by the polymer (Figure 4b). This is mainly due to the tumbling dynamics observed in shear flow; an individual trajectory for a molecule in shear flow explores a wide range of molecular extension as a molecule stretches, tumbles, collapses, and restretches.[48,49] Therefore, our results suggest that the application of nonequilibrium work relations to molecules in shear flow allows for the determination of the free energy landscape of the molecule well-beyond its average molecular extension in flow.

Finally, we can combine both stratification strategies to determine the stored elastic energy of the molecule for even higher energies as shown in Figure 5. Here, we apply successive

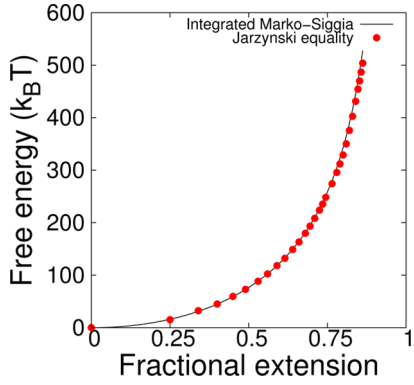

Figure 5. Equilibrium free energy landscape from multibead−spring model with fluctuating HI for λ-DNA in extensional flow. In this case, polymer molecules are initialized at an equilibrium average extension and are stretched by extensional flow using both stratification strategies.

and large steps in flow strength to stretch the molecule between nonequilibrium steady-states, akin to stratification strategy I. Within each large step in flow strength, the work done by the fluid on the polymer is determined as the molecule transitions between predefined molecular extensions which prescribes the subprocess, akin to stratification strategy II. On the basis of the work distribution for each subprocess, the free energy change between molecular extensions is calculated by applying the JE. The combination of both stratification strategies allows for efficient determination of the free energy landscape of the molecule. Furthermore, in all cases (Figures 3−5), once the free energy landscape is determined, chain elasticity can easily be calculated as the derivative of the energy with respect to molecular extension.[1]

Housekeeping Power. Housekeeping power (or applied power) is defined as the rate of work required for the fluid to maintain a polymer molecule at a constant average steady-state extension in flow. In this way, the fluid continues to perform work on a polymer in order to maintain a nonequilibrium steady-state. In brief, we calculate the transient work beyond the first time a molecule reaches its target predefined steady-state extension for several flow strengths in shear flow (Figure 6) and planar extensional flow (Figure 7). Transient work for single trajectories and the corresponding ensemble average work for λ-DNA modeled as a free-draining dumbbells stretched at $Wi = 0.45$ in shear and extensional flow are shown in Figures 6a and 7a, respectively. In both cases, we observe the average work increases linearly with time at long times. This indicates that the housekeeping power can be defined as:

$$P = \lim_{t\to\infty} \frac{d\langle W\rangle}{dt} \tag{20}$$

dx.doi.org/10.1021/ma400961s | Macromolecules 2013, 46, 8345−8355

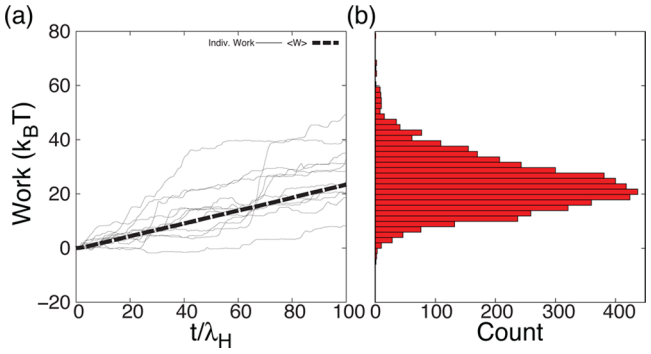

Figure 6. Housekeeping power for λ-DNA in shear flow at Wi = 0.45. (a) Transient individual (thin lines) work trajectories and ensemble average (thick line) work trajectory. (b) Jarzynski work distribution after ≈100 relaxation times.

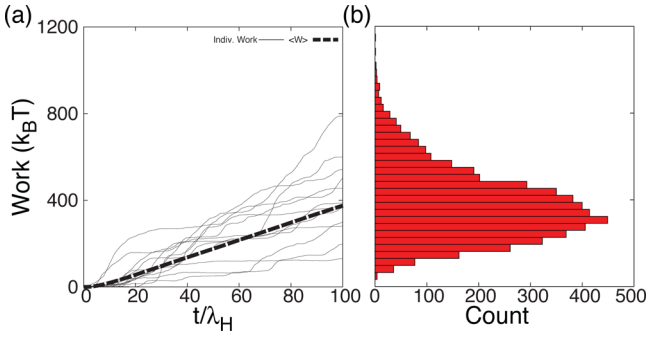

Figure 7. Housekeeping power for λ-DNA in extensional flow at Wi = 0.45. (a) Transient individual (thin lines) work trajectories and ensemble average (thick line) work trajectory. (b) Jarzynski work distribution after ≈100 relaxation times.

such that P is a nonzero constant in agreement with the predictions for steady-states maintained by nonconservative forces as in hydrodynamic flows.[51]

In order to deepen our understanding of the nature of the housekeeping power, we investigated more closely the work distributions in linear flows. Figures 6b and 7b show the corresponding work distribution after ≈100 relaxation times in shear flow and extensional flow. In the case of shear flow, we observe a near Gaussian work distribution, which indicates that the average state of molecule is near "equilibrium" at this flow strength (Figure 6b).[23] Indeed, a near Gaussian work distribution might be expected because the molecule remains (on average) in the compact configuration in shear flow at Wi = 0.45. However, a small fraction of trajectories exhibit negative work values in shear flow, which is a striking feature of the work distribution. Negative work corresponds to trajectories in which a molecule spends more time contracting than stretching, which is plausible in weak shear flow due to vorticity. However, we do not observe any trajectories with negative work values for polymers in extensional flow at Wi = 0.45, as shown in Figure 7b. Extensional flow is a strong flow with the ability to induce highly stretched polymer conformations in flow, which generally results in the molecule undergoing significantly more stretching events relative to contraction events. In addition, we observe that the average transient work in extensional flow is an order of magnitude larger than in shear flow at Wi = 0.45. In extensional flow, a polymer chain will be stretched to (on average) a higher molecular extension compared to shear flow; therefore, the fluid performs more work to maintain the average steady-state in extensional flow relative to shear.

Figure 8 shows the transient average work at different flow strengths for λ-DNA modeled as a free-draining dumbbell in

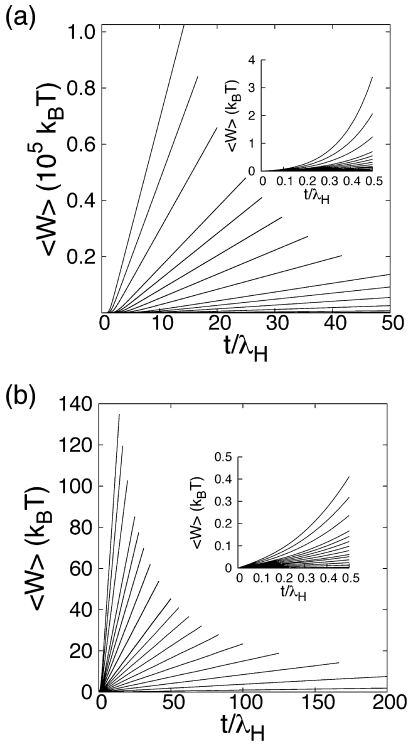

Figure 8. Transient average work in housekeeping power simulations at flow strengths ranging from Wi = 0.09 to 900. (a) Free-draining dumbbell model of λ-DNA in planar extensional flow. (b) Free-draining dumbbell model of λ-DNA in shear flow.

planar extensional flow (Figure 8a) and shear flow (Figure 8b). The insets in parts a and b of Figure 8 show the transient average work at short times. In both cases, we observe that the average transient work is nonlinear at short times, thereby indicating that the average steady-state has not be reached. However, in all cases, we observe a linear increase in the average transient work at long times, indicative of an average steady-state maintained by nonconservative forces. The slope of a transient average work trajectory yields the housekeeping power for the corresponding flow strength.

Housekeeping power as a function of flow strength for λ-DNA is shown in Figure 9. We determined housekeeping power for nonfree-draining behavior of λ-DNA using multi-bead−spring models with fluctuating HI. In this case, we show housekeeping power in units of k_BT/τ_R, which is the ratio of thermal energy to the relaxation time of the molecule. We observe clear power-law scalings of housekeeping power as a function of flow strength, and we determine the scaling exponent in different flow regimes for the non-free-draining chains. On the basis of the scaling exponents, we observe that the inclusion of HI plays a fairly insignificant role in the relationship between the housekeeping power and flow strength, especially at higher flow strengths when compared with the free-draining scalings.[1]

Furthermore, we systematically investigate the fundamental relationship between housekeeping power (P) and molecular weight (M) or number of Kuhn segments (N_K) at a given

dx.doi.org/10.1021/ma400961s | Macromolecules 2013, 46, 8345−8355

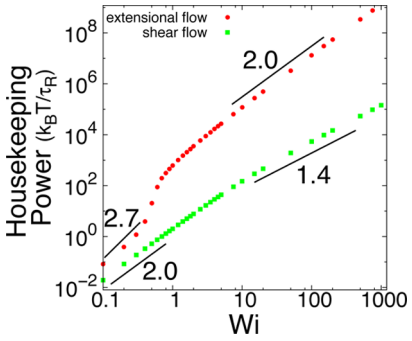

Figure 9. Housekeeping power as a function of flow strength for λ-DNA with hydrodynamic interactions in linear flows.

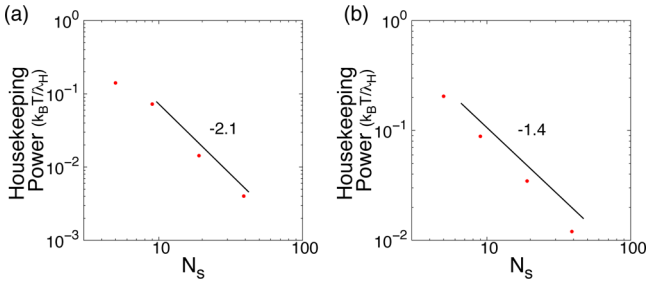

Figure 10. Relationship between housekeeping power and chain size (number of springs, N_s) for dsDNA in a shear flow at Wi = 0.7. Multibead−spring chains (a) with no hydrodynamic interactions and (b) with hydrodynamic interactions.

temperature and Weissenberg number. In determining this relationship, we first consider the simple case of Rouse chains in a shear flow. In particular, we note that for such a system, the polymer contribution to the viscosity (η_p) is given as[3]

$$\eta_p = nk_BT\frac{\zeta}{4H}\left(\frac{N_b^2 - 1}{3}\right) \tag{21}$$

where n is the number density of polymer chains. Furthermore, based on our recent work,[1] the housekeeping power is related to η_p simply through $P = \dot{\gamma}^2\eta_p$. The development of this relationship is based on the Kramers-Kirkwood expression for the stress tensor, noting that the housekeeping power is directly related to the nonisotropic contribution of the polymer to the solution viscosity.[1] On the basis of this relationship, the Rouse scaling for the longest relaxation time in the long chain limit ($N_b \approx N_s \gg 1$), and eq 21, we can express a simple scaling relation for the housekeeping power for a single Rouse chain in shear flow as:

$$P \sim \frac{k_BT}{\lambda_H}Wi^2N_b^{-2} \tag{22}$$

Using eq 22, we find that $P \sim Wi^2$ for a Rouse chain in shear flow, which is in good agreement with the simulation results at weak shear flows.[1] In addition, based on the relationship established in eq 22, we observe that for a constant Wi in the long chain limit, $P \sim N_K^{-2}$. This result establishes the scaling relationship between P and N_K for Rouse chains in shear flow. We note that this relationship is expected because at a constant Wi, the other longest available time scale is the relaxation time τ_R, and a dimensional analysis suggests that $P \sim \tau_R^{-1}$. Despite this analysis, there is still need for a detailed analytical theory that connects housekeeping power to polymer chain size.

Finally, beyond the analysis of Rouse chains in shear flow and in order to validate our proposed scalings, we performed simulations to determine the relationship between the housekeeping power and chain size for dsDNA molecules. We achieved this by determining the housekeeping power from our simulations at a fixed Wi for chains with different contour lengths such that the number of springs (N_s) is varied while the number of Kuhn segments per spring ($N_{K,s}$) is held constant. Using this approach, our results for long dsDNA molecules in shear flow at Wi = 0.7 modeled without and with hydrodynamic interactions and in the long chain limit, we find that $P \sim N_s^{-2.1}$ for no HI, and $P \sim N_s^{-1.4}$ for HI as shown in Figure 10, parts a and b, respectively. These scaling results are in good agreement with our proposed scalings based on a dimensional analysis noting Rouse and Zimm dynamics. Overall, from a polymer processing perspective, these results suggests that more housekeeping energy per time is required to maintain lower molecular weight polymers at an average steady-state at a given Wi. Furthermore, this energetic effect is less pronounced for truly flexible polymers where hydrodynamic interactions are dominant.

CONCLUSIONS

In this work, we demonstrate the general utility of applying nonequilibrium work relations via the Jarzynski equality to the dynamics of polymer chains in flow. In particular, we employ coarse-grained dumbbell and multibead−spring models for polymers with fluctuating HI to directly determine the stored elastic energy from far-from-equilibrium dynamics. We further demonstrate that our framework for determining materials properties can be applied to linear flows with or without vorticity. In addition, we investigate the inclusion of hydrodynamic interactions on the Jarzynski formalism in the context of housekeeping power defined as the energy expended by the fluid per time required to maintain a molecule at steady-state. Our findings suggest that the inclusion of HI does not affect the relationship between the housekeeping power and the applied flow strength. Finally, we derive simple relationships that connect the housekeeping power to polymer molecular weight in the Rouse and Zimm limits.

Our framework to determine the elastic energy from stretching trajectories of single polymers in flow can also serve as a validation tool for simulation techniques employed by rheologists. Indeed, our results demonstrate that coarse-grained models of polymers, as are commonly used in Brownian dynamics simulations, are thermodynamically self-consistent in the context of nonequilibrium work theorems. Beyond this, by relating the Jarzynski work to the housekeeping power in flowing dilute polymer solutions at steady-state, we provide a formalism to further distinguish between shear and extensional flows, and free-draining and non-free-draining behavior of polymers in terms of energy dissipation. In this way, we believe that nonequilibrium work relations present a powerful set of tools to investigate and deepen our understanding of soft materials in highly nonequilibrium flows.

AUTHOR INFORMATION

Corresponding Author

*(C.M.S.) E-mail: cms@illinois.edu.

Notes

The authors declare no competing financial interest.

■ ACKNOWLEDGMENTS

This work was supported by a Packard Fellowship from the David and Lucile Packard Foundation and an NSF CAREER Award (CBET 1254340) to C.M.S. and a Dow Chemical Company Fellowship in Chemical Engineering and an Illinois Computational Science and Engineering Fellowship to F. L.

■ REFERENCES

(1) Latinwo, F.; Schroeder, C. M. Submitted for publication in *Soft Matter*.
(2) Larson, R. G. *The Structure and Rheology of Complex Fluids*; Oxford University Press: Oxford, U.K., 1999.
(3) Bird, R. B.; Curtis, C. F.; Armstrong, R. C.; Hassager, O. *Dynamics of Polymeric Liquids*, 2nd ed.; Wiley: New York, 1987; Vol. 2.
(4) Shaqfeh, E. *J. Non-Newton. Fluid Mech.* **2005**, *130*, 1−28.
(5) Fuller, G. G.; Leal, L. G. *Rheol. Acta* **1980**, *19*, 580.
(6) Menasveta, M. J.; Hoagland, D. A. *Macromolecules* **1991**, *24*, 3427.
(7) Lee, E. C.; Muller, S. J. *Macromolecules* **1999**, *32*, 3295.
(8) Smith, D. E.; Babcock, H. P.; Chu, S. *Science* **1999**, *283*, 1724.
(9) Perkins, T. T.; Smith, D. E.; Chu, S. *Science* **1997**, *276*, 2016.
(10) Schroeder, C. M.; Shaqfeh, E. S. G.; Chu, S. *Macromolecules* **2004**, *37*, 9242−9256.
(11) Babcock, H. P.; Teixeira, R. E.; Hur, J. S.; Shaqfeh, E. S. G.; Chu, S. *Macromolecules* **2003**, *36*, 4544.
(12) Neuman, K.; Lionnet, T.; Allemand, J.-F. *Ann. Rev. Mater. Res.* **2007**, *37*, 33−67.
(13) de Gennes, P.-G. *J. Chem. Phys.* **1974**, *60*, 5030−5042.
(14) de Gennes, P.-G. *Scaling Concepts in Polymer Physics*; Cornell University Press: Ithaca, NY, 1979.
(15) Jarzynski, C. *Annu. Rev. Condens. Matter Phys.* **2011**, *2*, 329−351.
(16) Hummer, G.; Szabo, A. *Proc. Natl. Acad. Sci. U.S.A.* **2001**, *98*, 3658−3661.
(17) Jarzynski, C. *Phys. Rev. Lett.* **1997**, *78*, 2690−2693.
(18) Jarzynski, C. *Phys. Rev. E* **1997**, *56*, 5018−5035.
(19) Hatano, T.; Sasa, S.-i. *Phys. Rev. Lett.* **2001**, *86*, 3463−3466.
(20) Hatano, T. *Phys. Rev. E* **1999**, *60*, R5017−R5020.
(21) Hermans, J. *J. Phys. Chem.* **1991**, *95*, 9029−9032.
(22) Speck, T.; Seifert, U. *Phys. Rev. E* **2004**, *70*, 066112.
(23) Park, S.; Khalili-Araghi, F.; Tajkhorshid, E.; Schulten, K. *J. Chem. Phys.* **2003**, *119*, 3559−3566.
(24) Liphardt, J.; Dumont, S.; Smith, S. B.; Tinoco, I.; Bustamante, C. *Science* **2002**, *296*, 1832−1835.
(25) Gupta, A. N.; Vincent, A.; Neupane, K.; Yu, H.; Wang, F.; Woodside, M. T. *Nat. Phys.* **2011**, *7*, 631−634.
(26) Greenleaf, W. J.; Frieda, K. L.; Foster, D. A. N.; Woodside, M. T.; Block, S. M. *Science* **2008**, *319*, 630−633.
(27) Shank, E. A.; Cecconi, C.; Dill, J. W.; Marqusee, S.; Bustamante, C. *Nature* **2010**, *465*, 637−U134.
(28) Collin, D.; Ritort, F.; Jarzynski, C.; Smith, S.; Tinoco, I.; Bustamante, C. *Nature* **2005**, *437*, 231−234.
(29) Harris, N. C.; Song, Y.; Kiang, C.-H. *Phys. Rev. Lett.* **2007**, *99*, 068101.
(30) Mukamel, S. *Phys. Rev. Lett.* **2003**, *90*, 170604.
(31) Esposito, M.; Harbola, U.; Mukamel, S. *Rev. Mod. Phys.* **2009**, *81*, 1665−1702.
(32) Quan, H. T.; Jarzynski, C. *Phys. Rev. E* **2012**, *85*, 031102.
(33) Campisi, M.; Talkner, P.; Hänggi, P. *Phys. Rev. Lett.* **2009**, *102*, 210401.
(34) Heyl, M.; Kehrein, S. *Phys. Rev. Lett.* **2012**, *108*, 190601.
(35) Jendrejack, R. M.; de Pablo, J. J.; Graham, M. D. *J. Chem. Phys.* **2002**, *116*, 7752−7759.
(36) Schroeder, C. M.; Babcock, H. P.; Shaqfeh, E. S. G.; Chu, S. *Science* **2003**, *301*, 1515−1519.
(37) Latinwo, F.; Schroeder, C. M. *Soft Matter* **2011**, *7*, 7907−7913.
(38) Smith, D. E.; Perkins, T. T.; Chu, S. *Macromolecules* **1996**, *29*, 1372−1373.
(39) Rubinstein, M.; Colby, R. H. *Polymer Physics*; Oxford University Press: New York, 2003.
(40) Jendrejack, R. M.; Dimalanta, E. T.; Schwartz, D. C.; Graham, M. D.; de Pablo, J. J. *Phys. Rev. Lett.* **2003**, *91*, 038102.
(41) Khare, R.; Graham, M. D.; de Pablo, J. J. *Phys. Rev. Lett.* **2006**, *96*, 224505.
(42) Graham, M. D. *Annu. Rev. Fluid Mech.* **2011**, *43*, 273−298.
(43) Tree, D. R.; Wang, Y.; Dorfman, K. D. *Phys. Rev. Lett.* **2012**, *108*, 228105.
(44) Sharma, R.; Cherayil, B. J. *Phys. Rev. E* **2011**, *83*, 041805.
(45) Winkler, R. G. *Phys. Rev. Lett.* **2006**, *97*, 128301.
(46) Huang, C.-C.; Sutmann, G.; Gompper, G.; Winkler, R. G. *Europhys. Lett.* **2011**, *93*, 54004.
(47) Lee, J. S.; Shaqfeh, E. S. G.; Muller, S. J. *Phys. Rev. E* **2007**, *75*, 040802.
(48) Schroeder, C. M.; Teixeira, R. E.; Shaqfeh, E. S. G.; Chu, S. *Phys. Rev. Lett.* **2005**, *95*, 018301.
(49) Doyle, P. S.; Ladoux, B.; Viovy, J.-L. *Phys. Rev. Lett.* **2000**, *84*, 4769−4772.
(50) Batchelor, G. K. *An Introduction to Fluid Dynamics*; Cambridge University Press: Cambridge, England, 2000.
(51) Speck, T.; Mehl, J.; Seifert, U. *Phys. Rev. Lett.* **2008**, *100*, 178302.
(52) Speck, T. *The Thermodynamics of Small Driven Systems*. Ph.D. Dissertation, University of Stuttgart: Stuttgart, Germany, 2007.
(53) Turitsyn, K.; Chertkov, M.; Chernyak, V. Y.; Puliafito, A. *Phys. Rev. Lett.* **2007**, *98*, 180603.
(54) Hsieh, C.-C.; Li, L.; Larson, R. G. *J. Non-Newton. Fluid Mech.* **2003**, *113*, 147−191.
(55) Ottinger, H. C. *Stochastic Processes in Polymeric Fluids*; Springer Verlag: Berlin, 1996.
(56) Ermak, D. L.; McCammon, J. A. *J. Chem. Phys.* **1978**, *69*, 1352−1360.
(57) Marko, J. F.; Siggia, E. D. *Macromolecules* **1995**, *28*, 8759−8770.
(58) Cohen, A. *Rheol. Acta* **1991**, *30*, 270−273.
(59) Gore, J.; Ritort, F.; Bustamante, C. *Proc. Natl. Acad. Sci. U.S.A.* **2003**, *100*, 12564−12569.
(60) Somasi, M.; Khomami, B.; Woo, N. J.; Hur, J. S.; Shaqfeh, E. S. G. *J. Non-Newton. Fluid Mech.* **2002**, *108*, 227−255.
(61) Jendrejack, R. M.; Graham, M. D.; de Pablo, J. J. *J. Chem. Phys.* **2000**, *113*, 2894−2900.
(62) Press, W. H.; Flannery, B. P.; Teukolsky, S. A.; Vetterling, W. T. *Numerical Recipes in Fortran: The Art of Scientific Computing*, 2nd ed.; Cambridge University Press: Cambridge, U.K., 1992.
(63) Fixman, M. *Macromolecules* **1986**, *19*, 1204−1207.
(64) Hernandez-Ortiz, J. P.; de Pablo, J. J.; Graham, M. D. *J. Chem. Phys.* **2006**, *125*, 164906.
(65) Hernández-Ortiz, J. P.; de Pablo, J. J.; Graham, M. D. *Phys. Rev. Lett.* **2007**, *98*, 140602.
(66) Pohorille, A.; Jarzynski, C.; Chipot, C. *J. Phys. Chem. B* **2010**, *114*, 10235−10253.
(67) McQuarrie, D. A. *Statistical Mechanics*, 2nd ed.; University Science Books: Herndon, VA, 2000.
(68) Jendrejack, R. M.; de Pablo, J. J.; Graham, M. D. *J. Chem. Phys.* **2002**, *116*, 7752−7759.